

## LYMPHOID NEOPLASIA

## Evaluation of the potential therapeutic benefits of macrophage reprogramming in multiple myeloma

Alejandra Gutiérrez-González,<sup>1</sup> Mónica Martínez-Moreno,<sup>2</sup> Rafael Samaniego,<sup>1</sup> Noemí Arellano-Sánchez,<sup>2</sup> Laura Salinas-Muñoz,<sup>1</sup> Miguel Relloso,<sup>1</sup> Antonio Valeri,<sup>3</sup> Joaquín Martínez-López,<sup>3</sup> Ángel L. Corbí,<sup>2</sup> Andrés Hidalgo,<sup>4</sup> Ángeles García-Pardo,<sup>2</sup> Joaquín Teixidó,<sup>2</sup> and Paloma Sánchez-Mateos<sup>1</sup>

<sup>1</sup>Section of Immuno-oncology, Instituto de Investigación Sanitaria Gregorio Marañón, Complutense University School of Medicine, Madrid, Spain;

<sup>2</sup>Department of Cellular and Molecular Medicine, Centro de Investigaciones Biológicas, Madrid, Spain; <sup>3</sup>Section of Hematology, Hospital Universitario 12 de Octubre, Madrid, Spain; and <sup>4</sup>Area of Cell and Developmental Biology, Fundación Centro Nacional de Investigaciones Cardiovasculares, Madrid, Spain

## Key Points

- We report strategies to reprogram macrophages as a novel approach to treat MM mouse models using pro-M1 and blocking M2 signals.
- MIF is upregulated in the bone marrow microenvironment of MM patients and plays an autocrine role in protumoral MØ polarization.

**Tumor-associated macrophages (TAM) are important components of the multiple myeloma (MM) microenvironment that support malignant plasma cell survival and resistance to therapy. It has been proposed that macrophages (MØ) retain the capacity to change in response to stimuli that can restore their antitumor functions. Here, we investigated several approaches to reprogram MØ as a novel therapeutic strategy in MM. First, we found tumor-limiting and tumor-supporting capabilities for monocyte-derived M1-like MØ and M2-like MØ, respectively, when mixed with MM cells, both in vitro and in vivo. Multicolor confocal microscopy revealed that MM-associated MØ displayed a predominant M2-like phenotype in the bone marrow of MM patient samples, and a high expression of the pro-M2 cytokine macrophage migration inhibitory factor (MIF). To reprogram the protumoral M2-like MØ present in MM toward antitumoral M1-like MØ, we tested the pro-M1 cytokine granulocyte–macrophage colony-stimulating factor (GM-CSF) plus blockade of the M2 cytokines macrophage colony-stimulating factor or MIF. The combination of GM-CSF plus the MIF inhibitor 4-iodo-6-phenyl-pyrimidine achieved the best reprogramming responses toward an M1 profile, at both gene and protein expression**

**levels, as well as remarkable tumoricidal effects. Furthermore, this combined treatment elicited MØ-dependent therapeutic responses in MM xenograft mouse models, which were linked to upregulation of M1 and reciprocal downregulation of M2 MØ markers. Our results reveal the therapeutic potential of reprogramming MØ in the context of MM. (*Blood*. 2016;128(18):2241-2252)**

## Introduction

Multiple myeloma (MM) is an incurable hematologic neoplasia characterized by accumulation in the bone marrow (BM) of malignant plasma cells that produce monoclonal proteins and cause bone lesions, renal disease, and immunodeficiency.<sup>1</sup> Survival of malignant plasma cells is supported by interactions with the BM microenvironment (cells, extracellular matrix, and soluble factors), where macrophages (MØ) represent an important component.<sup>2,3</sup> Tumor-associated macrophages (TAM) and related myeloid-derived suppressor cells protect MM cells from spontaneous and chemotherapy-induced apoptosis and provide an immunosuppressive microenvironment.<sup>4,5</sup> In addition, TAM participate in complex paracrine loops with stromal and endothelial cells, promoting MM survival and angiogenesis through release of vascular endothelial growth factor and vasculogenic mimicry.<sup>6-8</sup> Indeed, several studies have shown that MM patients with high BM-MØ infiltration have poor prognosis.<sup>9,10</sup> Despite their protumoral actions, MØ in the myeloma niche display inherent tumoricidal potential, as demonstrated by the use of anti-CD47 antibodies that block “don’t eat me” signals and elicit MØ-mediated myeloma regression.<sup>11</sup> Moreover, T-helper 1–activated MØ are important effectors cells mediating antitumor CD4<sup>+</sup>

T-cell responses in myeloma models.<sup>12</sup> Interestingly, macrophage-activating immunotherapy using CD40 plus Toll-like receptor ligation has shown clinical benefit in a MM murine model.<sup>13</sup>

MØ therefore have great plasticity and can differentiate into several functional states in response to microenvironmental signals.<sup>14</sup> Using different activation stimuli in vitro, MØ have been classified into 2 major polarized states: M1-MØ refers to classically activated MØ by cytokines such as interferon- $\gamma$  (IFN- $\gamma$ ), tumor necrosis factor- $\alpha$  (TNF- $\alpha$ ), or granulocyte–macrophage colony-stimulating factor (GM-CSF), whereas M2-MØ refers to alternatively activated MØ by interleukin-4 (IL-4), IL-13, or IL-10.<sup>15</sup> M1-MØ have remarkable tumoricidal activity through secretion of cytotoxic factors (type I interferons, TNF- $\alpha$ , reactive nitrogen/oxygen species) and phagocytosis.<sup>16,17</sup> Notably, M1-MØ can initiate specific antitumor immune responses through high expression of the major compatibility complex and costimulatory molecules for efficient antigen presentation and proinflammatory cytokines (IL-12 and IL-23) to stimulate cytotoxic T and natural killer cells.<sup>18</sup> In contrast, M2-MØ generally show low reactive nitrogen/oxygen species production and low antigen-presentation and suppress antitumor immunity.<sup>19</sup>

Submitted 26 January 2016; accepted 4 September 2016. Prepublished online as *Blood* First Edition paper, 13 September 2016; DOI 10.1182/blood-2016-01-695395.

The online version of this article contains a data supplement.

The publication costs of this article were defrayed in part by page charge payment. Therefore, and solely to indicate this fact, this article is hereby marked “advertisement” in accordance with 18 USC section 1734.

© 2016 by The American Society of Hematology

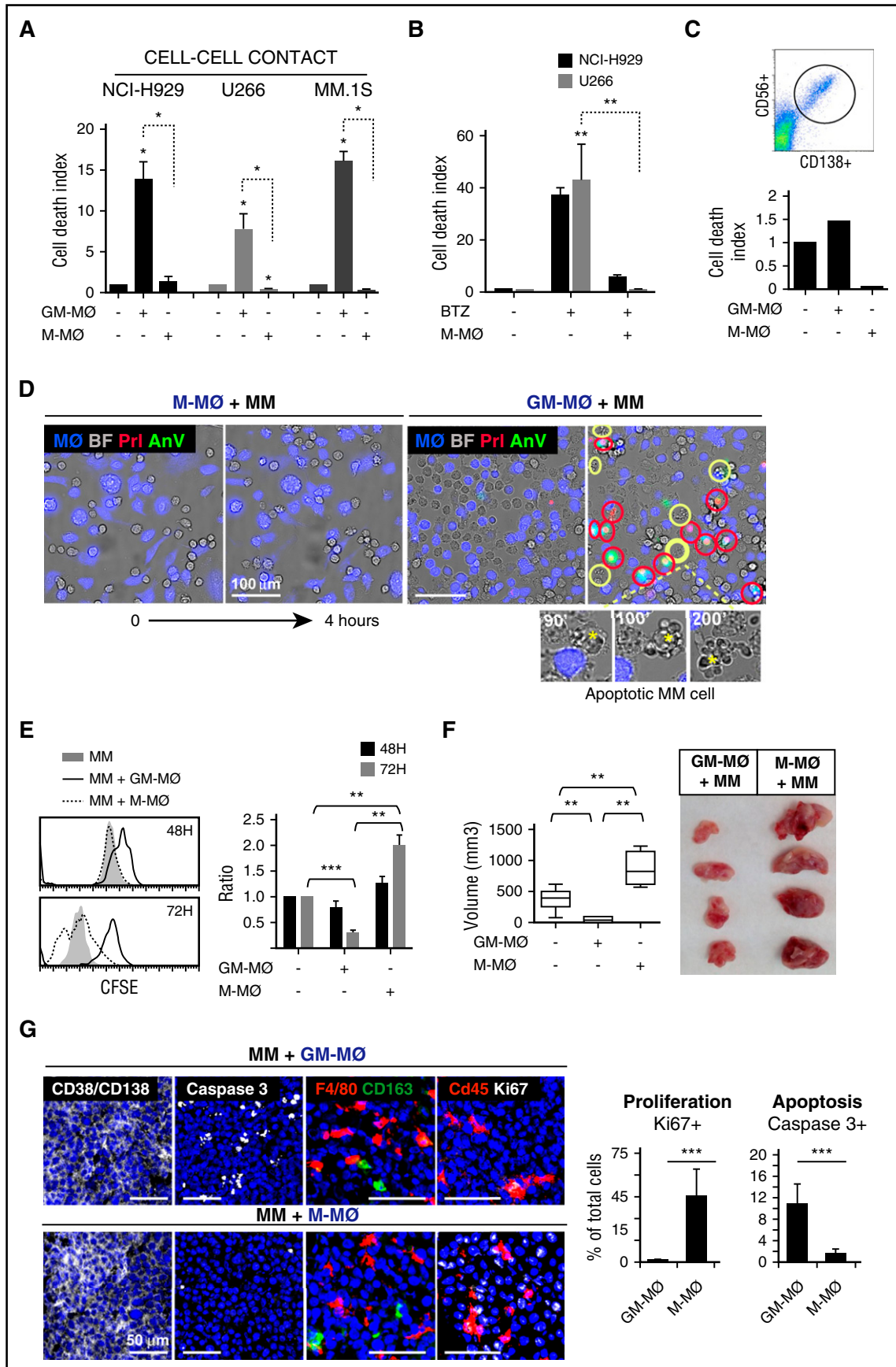


**Figure 1.** M1-MØ are cytotoxic to MM cells and inhibit MM cell proliferation and tumor development in vivo. (A) The indicated MM cell lines were cultured alone or in the presence of GM-MØ or M-MØ for 3 days. Cell death was measured and normalized by MM cell spontaneous death. Data represent mean ± standard error of the mean (SEM) of 6 independent experiments with different MØ donors. (B) MM cells were cultured for 72 hours in the absence or presence of M-MØ, and cell death was induced with

Current *in vivo* evidence indicates that TAM are predominantly polarized toward the M2-like phenotype in advanced cancer stages, and that MØ targeting can be clinically beneficial.<sup>14,19,20</sup> Rather than depletion of TAM, more targeted therapies are directed to block the protumor functions of TAM, while promoting their antitumor activities.<sup>21</sup> Such reprogramming from M2-like to M1-like MØ may control inflammation-related cancer progression and elicit tumor-destructive reactions. Several factors can induce the M2-MØ phenotype, including macrophage-colony stimulating factor (M-CSF) and macrophage migration inhibitory factor (MIF), both abundantly produced in tumors.<sup>20,22,23</sup> M-CSF is crucial for MØ differentiation and survival and inhibition of its signaling ablates TAM in mouse tumor models and is associated with clinical benefit in patients.<sup>20,24</sup> MIF is strongly upregulated in tumors and is related to tumor progression and high clinical stage.<sup>25,26</sup> Furthermore, MIF-deficient models of melanoma and chronic lymphocytic leukemia displayed prolonged survival.<sup>22,27</sup>

In this study, we have characterized the functions of M1-MØ compared with M2-MØ in MM and have explored possible therapeutic protocols targeting MØ in myeloma. Using a new double strategy that combines GM-CSF and antagonizes MIF signaling, we have reprogrammed TAM and showed therapeutic benefit in MM xenograft models. Furthermore, we have defined the role of MIF and its receptors, CD74 and CXCR7, in M2-MØ polarization.

## Materials and methods

### Patient samples, MØ, and MM cell lines

Samples from MM patients were obtained after informed consent and followed the guidelines from the Ethics Committees of Instituto de Investigación Sanitaria Gregorio Marañón, Hospital 12 de Octubre, and Consejo Superior de Investigaciones Científicas. Patient characteristics are reported in supplemental Table 1, available on the *Blood* Web site. CD138<sup>+</sup> primary myeloma cells were purified from the mononuclear fraction of BM samples from patients with active MM using CD138 microbeads (Miltenyi Biotec, Bergisch Gladbach, Germany). Human monocytes were purified from buffy coats and differentiated to M1-like or M2-like MØ using GM-CSF or M-CSF, respectively, as previously reported<sup>28</sup> (protocol in supplemental Figure 1E). Hereafter, we will refer to these phenotypes as GM-MØ and M-MØ, respectively. Human MØ and MM cell lines (NCI-H929, U266, MM.1S, and MM.1S-GFP) were maintained in Roswell Park Memorial Institute 1640 medium/10% fetal calf serum (Sigma-Aldrich, St. Louis, MO) at 37°C in 5% CO<sub>2</sub>/95% air atmosphere.

For M-MØ reprogramming, the supernatant of previously differentiated M-MØ was replaced with fresh medium containing reprogramming agents (provided in supplemental Table 2) every 2 days for 7 additional days, as indicated in reprogramming protocol (supplemental Figure 2A).

### MØ and MM cell cocultures

MM cells were cocultured with GM-MØ, M-MØ, or reprogrammed MØ at 1:1 MØ/MM ratio. After 3 days, MM cell death was analyzed by flow cytometry, using the Annexin V/Propidium Iodide Kit (BD Bioscience,

San Jose, CA). Staining with CD14Ab was used to exclude MØ from the analysis. MM cell proliferation was measured using carboxyfluorescein diacetate succinimidyl ester (CFSE; Life Technologies), and MØ and dead cells were excluded from this analysis using CD14Ab and 7-aminoactinomycin D staining, respectively.

For non-cell-cell contact experiments, MØ were differentiated in the lower chamber of 0.4- $\mu$ m pore size Transwell inserts. MM cells were added to the upper chamber of the insert, and MM cell death was determined after 3 days of culture. For experiments with conditioned media, the supernatants from various types of MØ or from GM-MØ+MM cocultures were collected and added to MM cells (50% vol/vol). MM cell death analyses were performed after 3 days of culture. Conditioned media inactivation was performed by heating supernatants at 100°C during 10 minutes.

### Other methods

Other methods, reagents, and antibodies are provided in supplemental Methods and supplemental Table 3.

## Results

### Differential role of polarized MØ on MM cell survival, proliferation and tumor growth

To determine the tumoricidal potential of polarized MØ toward MM cells, human monocytes were treated with either GM-CSF or M-CSF, to generate M1-like (GM-MØ) and M2-like (M-MØ) MØ, respectively. Phenotypical analyses confirmed that M-MØ had higher protein or messenger RNA expression of the M2 markers CD163, folate receptor  $\beta$  (FR $\beta$ , encoded by *FOLR2*), *STAB1*, *SERPIN2*, and *CCL2*, and lower expression of the M1 markers ICAM3, *EGLN3*, *INHBA*, and *MMP12* than GM-MØ<sup>29-33</sup> (supplemental Figure 1A). GM-MØ and M-MØ from 6 independent donors were cocultured with several MM cell lines and subsequently analyzed by flow cytometry, using annexin V and propidium iodide (AnV/PI) to identify dead MM cells and CD14 to exclude MØ (Figure 1A; representative MØ donor in supplemental Figure 1B). MM cells cocultured with GM-MØ showed enhanced cell death compared with MM cells cultured alone or cocultured with M-MØ (Figure 1A). M-MØ also supported resistance of MM cells to the cytotoxic agent bortezomib (Figure 1B). Moreover, M-MØ protected primary MM cells from spontaneous death in *ex vivo* cultures, whereas GM-MØ enhanced basal cell death by 50% (Figure 1C).

We next used video-microscopy to monitor MM cells in coculture with MØ. During the first hours of coculture with GM-MØ, a significant number of NCI-H929 MM cells showed either rapid AnV<sup>+</sup>/PI<sup>+</sup> staining (necrotic cell death) or long-lasting membrane blebbing and cell shrinkage (apoptotic cell death) (Figure 1D; supplemental Video 1), indicating that GM-MØ were able to induce both forms of programmed cell death. By contrast, there were no dead MM cells in M-MØ<sup>+</sup>MM cell cocultures or MM cells cultured alone (Figure 1D; supplemental Video 2).

**Figure 1 (continued)** bortezomib (10 nM) (n = 3 MØ donors). (C) Cell death analysis of patient CD138<sup>+</sup> MM BM cells (dot plot) cultured alone or with GM-MØ or M-MØ (48 hours). (D) NCI-H929 cells were cocultured with GM-MØ or M-MØ (stained with CFSE; blue) and live-imaged for 4 hours. First and last frames are shown (bright field images). Rapid acquisition of AnV (green)/PI (red) staining represents necrotic cells (red circles). Blebbing-apoptotic cells are circled in yellow, and one magnified case is indicated (asterisks). Scale bars, 100  $\mu$ m. (E) MM cell proliferation (CFSE dilution method) in the presence of GM-MØ or M-MØ. A representative experiment is shown on the left, and mean fluorescence intensity (MFI) values of 3 independent MØ donors normalized by NCI-H929 cultured alone are shown on the right. (F-G) NCI-H929 cells were injected (subcutaneously) alone or mixed with GM-MØ or M-MØ (1:1) in the flank of NSG mice. After 10 days, mice were sacrificed for tumor volume evaluation (F) and confocal microscopy analysis (G) by determining CD138/CD38, caspase 3, F4/80, CD163, and cd45, and Ki67 labeling. Scale bars, 50  $\mu$ m. Percentage of proliferating (Ki67) and apoptotic cells (active caspase 3) along intratumoral areas is represented on the right. Data show media  $\pm$  SEM of at least 4 mice per group. \**P* < .05; \*\**P* < .01; \*\*\**P* < .001. (D,G) Scale bars as indicated.

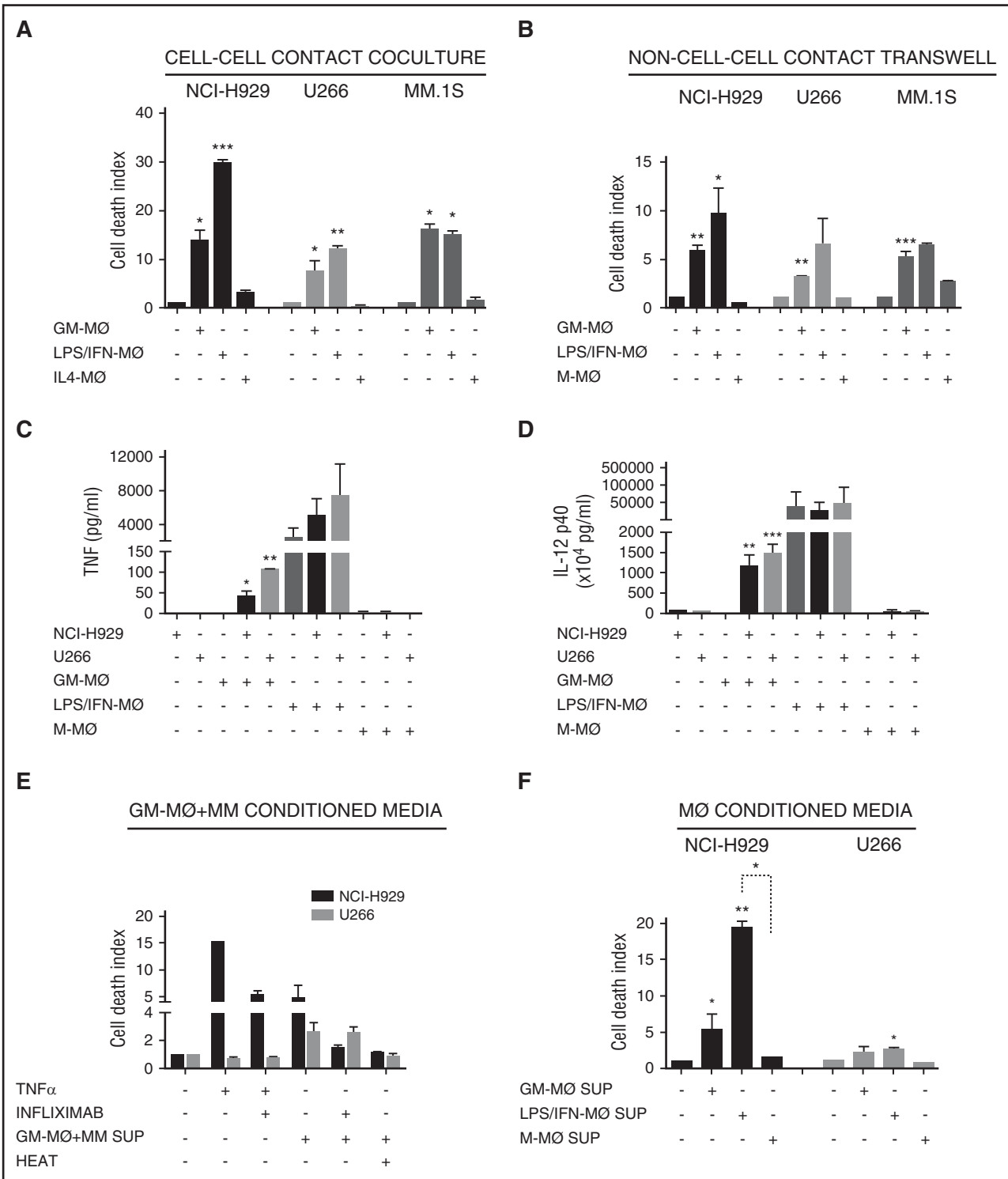


**Figure 2. M1-MØ and M2-MØ secretion of cytotoxic factors and cross-activation in coculture with MM cells.** (A-B) MM cell death was analyzed after 72 hours of coculture of MM cells alone or in the presence of various types of the indicated MØ, in cell-cell contact experiments (A) and non-cell-cell contact Transwell experiments (B). (C-D) Determination by enzyme-linked immunosorbent assay of TNF-α (C) and IL-12 p40 (D) levels in supernatants collected after 48 hours of culture of various types of the indicated MØ, MM cell lines, or MM+MØ cocultures. (E) NCI-H929 and U266 cells were cultured with TNF-α (200 ng/mL) or supernatants collected from GM-MØ+NCI-H929 and GM-MØ+U266 cocultures, respectively (measured in C), and treated with infliximab (80 μg/mL), as indicated. GM-MØ+MM conditioned media were inactivated by heat (10 minutes at 100°C). (F) Conditioned media of various types of the indicated MØ were collected and added to NCI-H929 or U266 cells (50% vol/vol). MM cell death was measured after 72 hours of culture. Summarized results of at least 3 independent experiments with different donors ± SEM are shown. \*P < .05; \*\*P < .01; \*\*\*P < .001.

To analyze the role of MØ on MM cell proliferation, we used CFSE dilution to monitor cell division of live MM cells (7-aminoactinomycin D-negative). Figure 1E shows a progressive decrease in cell

fluorescence in MM cells cocultured with M-MØ, indicating active MM cell proliferation. MM cells cocultured with GM-MØ maintained high CFSE-staining, whereas MM cells cultured alone showed

intermediate CFSE staining (Figure 1E). These results indicated that M2-M $\phi$  enhance cell proliferation, whereas M1-M $\phi$  do not.

We next used a MM cell–xenograft model to examine whether human M $\phi$  could impact tumor development. NCI-H929 cells were mixed with either GM-M $\phi$  or M-M $\phi$  and injected subcutaneously into NSG mice. Determination of tumor size revealed that MM cells coinjected with M-M $\phi$  developed larger tumors than when coinjected with GM-M $\phi$  (Figure 1F). MM cells injected alone developed intermediate-sized tumors. Tissue analysis revealed a major component of CD38<sup>+</sup>/CD138<sup>+</sup> tumor cells with scattered mouse and human M $\phi$  in both tumors (Figure 1G; quantified in supplemental Figure 1C). Interestingly, MM+GM-M $\phi$  tumors displayed enhanced active caspase 3 levels, whereas MM+M-M $\phi$  showed higher Ki67 staining, revealing inverse apoptosis/proliferation ratio in each tumor. Comparable results were obtained when either GM-M $\phi$  or M-M $\phi$  were injected into the tumor at a later stage (after tumor volume reached 100 mm<sup>3</sup>) (supplemental Figure 1D). These data indicate that M-M $\phi$  enhance and GM-M $\phi$  suppress MM tumor growth in vivo.

### Distinct response of polarized M $\phi$ in the secretion of cytotoxic factors and cross-activation by MM cells

To account for differences in macrophage differentiation protocols, we further exposed GM-M $\phi$  to lipopolysaccharide (LPS) and IFN- $\gamma$  (LPS/IFN-M $\phi$ ), whereas M-M $\phi$  were treated with IL-4 (IL4-M $\phi$ ) (see protocol in supplemental Figure 1E). LPS/IFN-M $\phi$  displayed enhanced tumoricidal effect toward NCI-H929, but not toward U266 and MM.1s cells, compared with GM-M $\phi$  (Figure 2A). These data indicate that further activation of GM-M $\phi$  with IFN- $\gamma$  and LPS potentiates their killer ability toward certain MM cell lines.

To determine whether the tumoricidal activity of M $\phi$  toward MM cells requires cell-cell contact, we used Transwell inserts to separate M $\phi$  and MM cells during culture. GM-M $\phi$ , and to a larger extent LPS/IFN-M $\phi$ , retained significant tumoricidal ability in this system, whereas M-M $\phi$  did not alter MM cell viability (Figure 2B). Furthermore, as Transwell inserts prevent phagocytosis, the data show that the differential behavior of GM-M $\phi$  and M-M $\phi$  was not due to their distinct ability to engulf apoptotic/necrotic cells. These results indicated that M $\phi$  tumoricidal effect involved, at least partially, the secretion of cytotoxic factors, a potential candidate being TNF- $\alpha$ .<sup>34</sup> No TNF- $\alpha$  production was detected in GM-M $\phi$ , M-M $\phi$ , or MM cell culture media (Figure 2C). Interestingly, coculture of GM-M $\phi$  with NCI-H929 or U266 MM cells induced TNF- $\alpha$  secretion, whereas no TNF- $\alpha$  was detected in cocultures of MM cells with M-M $\phi$ . Culture supernatants of activated LPS/IFN-M $\phi$  contained large amounts of TNF- $\alpha$ , and coculture with NCI-H929 or U266 MM cells further upregulated its secretion (Figure 2C). Production of IL-12 was also monitored as this cytokine encompasses both innate and adaptive antitumor immunity.<sup>35</sup> Similarly to TNF- $\alpha$ , GM-M $\phi$  did not produce IL-12, but this powerful antitumor cytokine was highly induced upon coculture with MM cells or activation by LPS/IFN (Figure 2D). These experiments demonstrated cross-activation of GM-M $\phi$  in coculture with MM cells, which induced production of TNF- $\alpha$  and IL-12, compared with the lack of these cytokines in M-M $\phi$  cocultured with MM cells. To further explore the role of TNF- $\alpha$  in M $\phi$ -dependent MM cell death, we incubated the supernatants obtained from Figure 2C with the TNF- $\alpha$ -blocking antibody (Ab) infliximab and performed cytotoxic assays with NCI-H929 or U266 cells (cell lines sensitive and resistant to TNF- $\alpha$ -induced cell death, respectively<sup>36</sup>). Figure 2E shows that infliximab reduced NCI-H929 cell death when cultured with

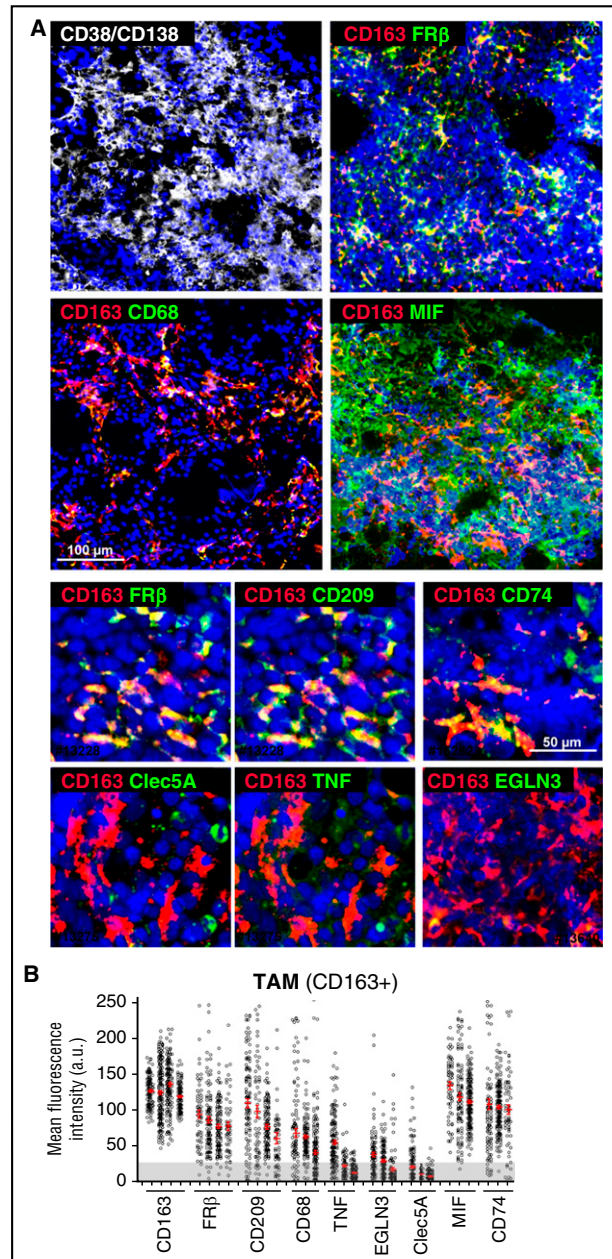


**Figure 3. Phenotyping of MM-M $\phi$  from BM patient samples.** (A) Multicolored staining of BM aspirates containing particles from active disease MM patients, CD38/CD138 (white), CD163 (red); FR $\beta$ , CD68, MIF, CD209, CD74, Clec5A, TNF, EGLN3 (green), as indicated. Upper panels represent panoramic views, whereas bottom panels are magnified ones. Nuclear 4',6-diamidino-2-phenylindole (DAPI) appears in blue in all cases. (B) Plot showing the MFI for each marker in CD163<sup>+</sup> TAM (n = 10 cases). Cells > 25 arbitrary units (a.u.) are considered positive, relative to negative control. Scale bars as indicated.

GM-M $\phi$ +MM cell supernatant. In contrast, U266 cells were killed by other cytotoxic factors sensitive to heat inactivation (Figure 2E).

To avoid M $\phi$ -MM cell cross-talk, we performed experiments with GM-M $\phi$  conditioned media, which still induced cell death of NCI-H929 cells and to a lesser extent of U266 cells (Figure 2F). LPS/IFN-M $\phi$  media enhanced death of NCI-H929 cells but not of U266 cells. Altogether, these data demonstrate the differential response of M1-like M $\phi$ , compared with M2-like M $\phi$ , to secrete IL-12, TNF- $\alpha$ , and other cytotoxic factors and to be cross-activated by MM cells.

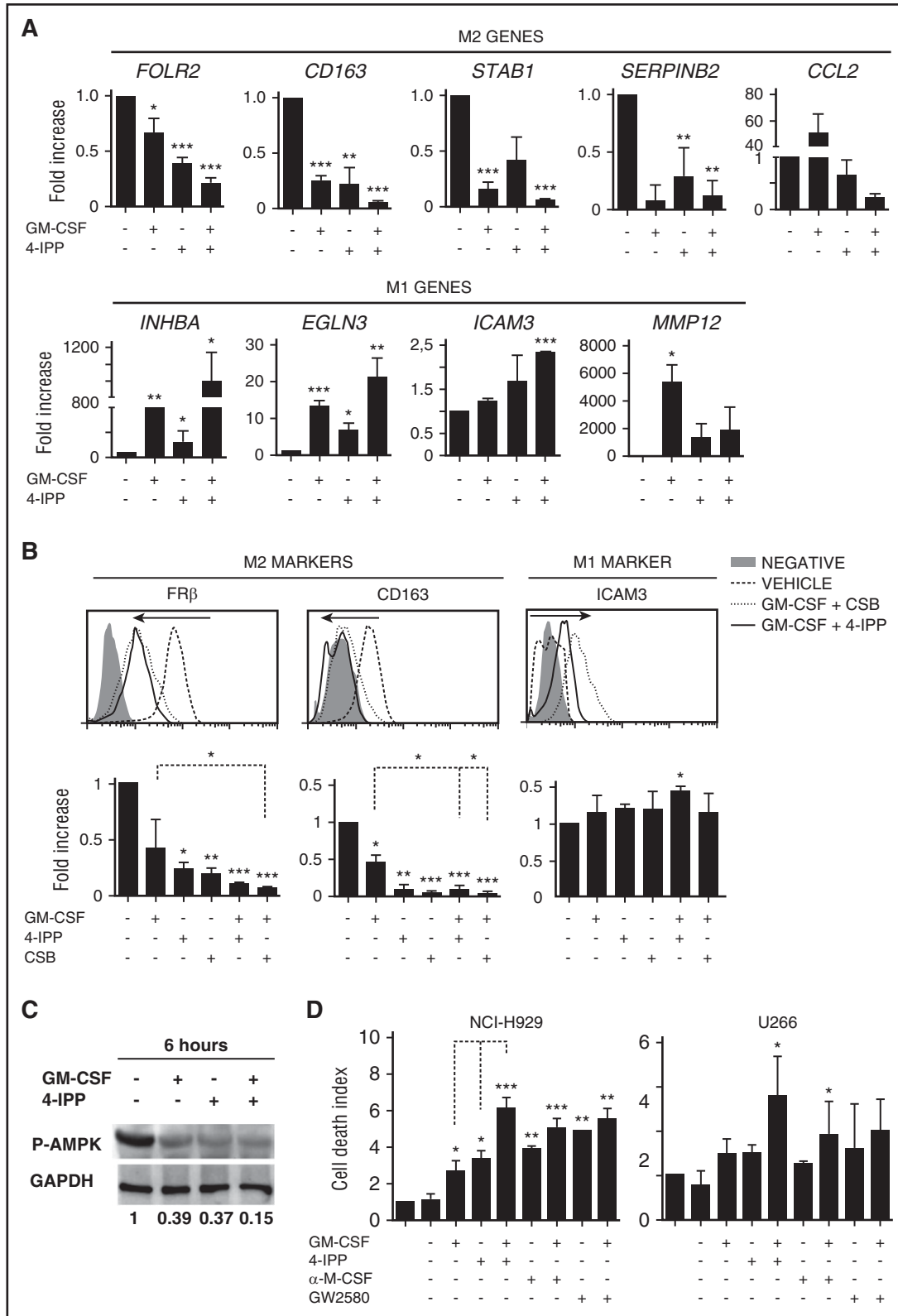


**Figure 4. Repolarization of protumoral M-MØ toward antitumoral MØ.** (A) Quantitative reverse transcription polymerase chain reaction (qRT-PCR) analyses of M2 and M1 genes from M-MØ treated for 24 hours with GM-CSF (1000 U/mL), the MIF inhibitor 4-IPP (50 μM), or in combination. Values of M-MØ in the absence of treatment are given an arbitrary value of 1. Results represent mean ± SEM of 10 independent donors. (B) Flow cytometry histograms showing cell surface expression of FRβ, CD163, and ICAM-3 in M-MØ untreated or treated as indicated. Results from a representative MØ donor (upper graphs), and MFI ± SEM quantification of at least 4 independent experiments with the indicated treatments (lower graphs) are shown. Values in the absence of treatment are given an arbitrary value of 1. (C) Immunoblot analysis of phospho-AMPK (P-AMPK) expression in M-MØ untreated or treated for 6 hours with GM-CSF, 4-IPP, or in combination. Densitometric analyses (a.u.) normalized to glyceraldehyde-3-phosphate dehydrogenase (GAPDH) levels and referred to M-MØ control are shown. (D) Determination of NCI-H929 and U266 cell death alone (first bar) or cultured with M-MØ untreated or treated as indicated. 4-IPP (50 μM), M-CSF neutralizing Ab (1 μg/mL), M-CSF inhibitor GW2580 (1 μM). Results represent mean ± SEM of 3 independent experiments with different donors. \**P* < .05; \*\**P* < .01; \*\*\**P* < .001.

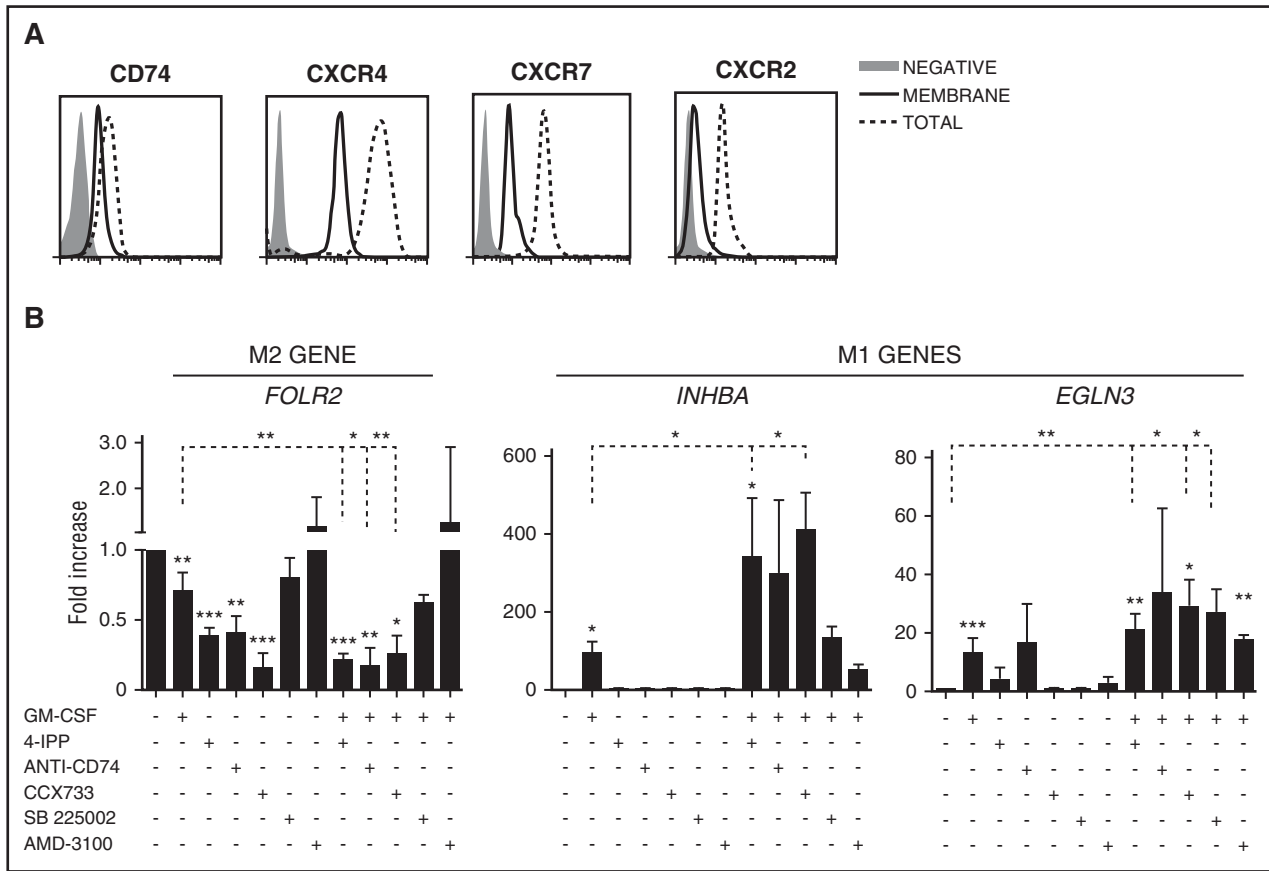


**Figure 5. MIF receptors and signaling during M0 repolarization.** (A) Flow cytometry analyses of intracellular and surface expression of MIF receptors CXCR4, CXCR7, CXCR2, and CD74 on M-M0. (B) Expression levels of *FOLR2*, *INHBA*, and *EGLN3*, as determined by qRT-PCR on M-M0 treated for 24 hours with GM-CSF (1000 U/mL); 4-IPP (50 μM); AMD3100 (25 μg/mL); CCX733 (100 nM); SB 225002 (300 nM) and α-CD74 blocking Ab (5 μg/mL); or GM-CSF in combination with all of them. Values in the absence of treatment are given an arbitrary value of 1. Result represents mean ± SEM of 4 independent donors. \**P* < .05; \*\**P* < .01; \*\*\**P* < .001.

**Expression of M0 polarization markers by MM-associated M0**

We next analyzed the in vivo polarization state of M0 present in BM samples, highly infiltrated by CD38<sup>+</sup>/CD138<sup>+</sup> plasma cells, from active MM patients. Whole mounts of BM samples were stained with M0 polarization markers and analyzed by confocal microscopy.<sup>37</sup> Initial identification of M0 was performed using a combination of CD68 and CD163 M0 markers (Figure 3A), finding high expression of CD163 and moderate expression of CD68 in MM-infiltrating M0 (Figure 3B). CD163<sup>+</sup> M0 were gated to quantify relative fluorescence expression of M1 markers CLEC5A, TNF-α, and EGLN3, and M2 markers CD209 and FRβ<sup>38</sup> (Figure 3A). We quantified >3000 single cells in several cases, and these analyses revealed that MM-associated M0 highly express CD163, CD209, and FRβ, whereas most M0 were negative for CLEC5A, TNF-α, and EGLN3 (Figure 3B). With respect to cytokines known to drive M2-TAM polarization, we found that MIF, a cytokine secreted by MM cells, was highly detected in the BM microenvironment. Interestingly, MM TAM showed elevated expression of CD74, MIF high-affinity receptor.<sup>39</sup>

**Protumoral toward antitumoral M0 reprogramming**

We then explored strategies to functionally reprogram established protumoral M0 into tumoricidal effector M0 by using pro-M1 stimuli in combination with blocking M2 autocrine/paracrine signaling and subsequently monitored expression of M1/M2 markers (see protocol

and M0 viability in supplemental Figure 2A-B). Treatment with GM-CSF alone induced upregulation of M1-associated genes and downregulation of most M2-associated genes (Figure 4A). However, the combination of GM-CSF with blockade of M2-signaling using an anti-M-CSF neutralizing Ab, or blocking the M-CSF receptor with GW2580 or Ki20227,<sup>40</sup> reduced the expression of M1 genes compared with GM-CSF treatment alone (supplemental Figure 2C).

It has been reported that MIF controls the alternative activation of tumor M0 in a melanoma mouse model,<sup>22</sup> and we found high expression of MIF in the BM microenvironment (Figure 3). Quantification of MIF secretion showed that is abundantly produced by M-M0 as well as by MM cells (supplemental Figure 2D). Therefore, our next strategy was to block autocrine/paracrine MIF production either with the suicide antagonist 4-iodo-6-phenyl-pyrimidine (4-IPP),<sup>41</sup> with the allosteric inhibitor p425, also known as Chicago Sky Blue 6B (CSB),<sup>42</sup> or by knocking down MIF using small interfering RNA. 4-IPP alone or MIF silencing significantly repressed M2-associated genes, which were further reduced by combining 4-IPP or CSB with GM-CSF (Figure 4A; supplemental Figure 2E-F). Furthermore, GM-CSF treatment showed a cooperative effect when combined with 4-IPP or CSB enhancing M1 genes, in contrast to M-CSF signaling antagonists. These changes were stable enough to downregulate the surface expression of FRβ and CD163 and to upregulate the M1 marker ICAM3 (Figure 4B).

In addition to changes in receptor surface expression, M0 polarization is associated with a shift in energy metabolism, and the

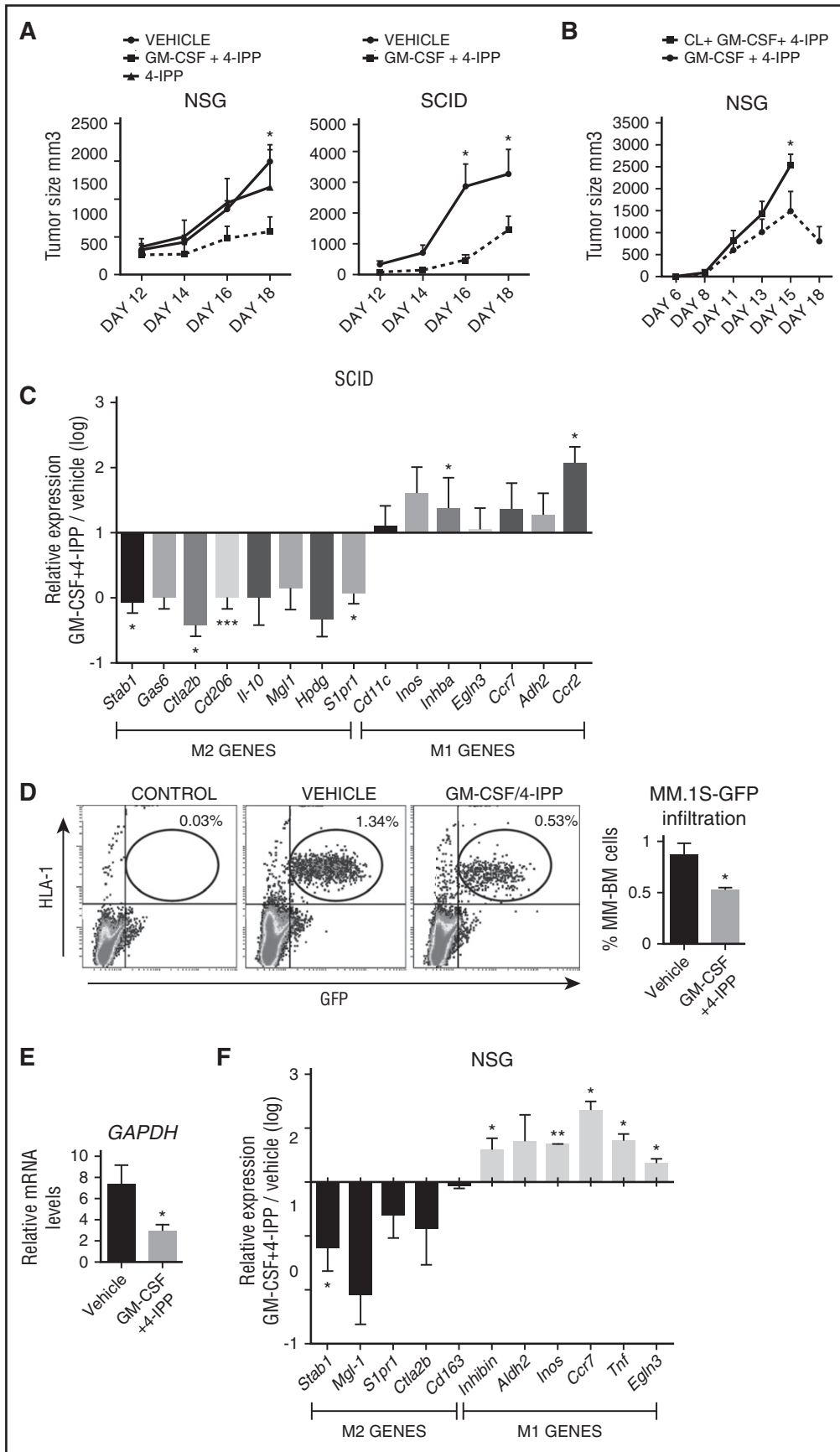


**Figure 6. GM-CSF+4-IPP therapeutic effect in immunodeficient mice MM xenograft models.** (A) NCI-H929 cells were inoculated subcutaneously into the flank of NSG (left graph) or SCID mice (right graph). When tumors reached volumes of 100 mm<sup>3</sup>, mice were treated every 2 days until sacrifice (day 18) with the indicated treatments (left,



adenosine 5'-monophosphate-activated protein kinase (AMPK) is central in this regulation.<sup>43</sup> To analyze AMPK activity during M-MØ reprogramming toward M1, we analyzed by western blot T172 phosphorylation levels linked to AMPK activation, which is higher in M-MØ than in GM-MØ (data not shown). Interestingly, treatment of M-MØ with either GM-CSF or 4-IPP decreased AMPK T172 phosphorylation, and reduction was even higher by combining both treatments (Figure 4C). These data indicate that GM-CSF and 4-IPP strongly downregulate AMPK activity in M-MØ, suggesting a pro-inflammatory metabolic shift that might favor their pro-inflammatory functions.<sup>44</sup>

We next determined the tumoricidal ability toward MM cells of MØ reprogrammed by different stimuli. M-MØ reprogrammed with GM-CSF, 4-IPP, or blocking M-CSF alone displayed significant tumoricidal ability. Notably, a remarkable increase in MM cell death was reached by reprogrammed MØ treated with the combination of GM-CSF plus inhibition of M-CSF or MIF signaling, which was also confirmed by video-microscopy (Figure 4D; supplemental Figure 2G-H). Nonetheless, the combination of GM-CSF+4-IPP showed the largest cytotoxic effect toward MM cells (Figure 4D). Altogether, these results indicate that the combination GM-CSF+4-IPP was remarkably effective at reprogramming M-MØ toward M1-like MØ, as assessed by gene and protein expression, as well as by tumoricidal responses. In addition, these results suggest that combining pro-M1 and anti-M2 treatments may synergize for a more efficient repolarization toward antitumoral M1-like MØ.

#### CD74 and CXCR7 are the MIF receptors involved in MØ reprogramming

Besides binding to the high-affinity receptor CD74, MIF interacts with the chemokine receptors CXCR4, CXCR7, and CXCR2.<sup>45</sup> To further characterize the role of MIF in MØ polarization, we first analyzed the expression of these receptors on M-MØ. These MØ highly expressed CXCR4 at the cell surface, whereas CXCR7, CXCR2, and CD74 showed a predominant intracellular distribution (Figure 5A). We next compared the ability of 4-IPP together with MIF receptor blocking antibodies or antagonists to reprogram M-MØ, alone or in combination with GM-CSF. Interestingly, the anti-CD74 Ab, the CXCR7-antagonist CCX733, and 4-IPP strongly reduced the expression of the M2-specific *FOLR2* gene (Figure 5B left). Blocking CXCR2 or CXCR4 was less effective, suggesting that MIF was preferentially signaling through CD74 and CXCR7 to repolarize M2 MØ. 4-IPP or the anti-CD74 Ab only mildly affected the expression of the M1 genes (Figure 5B). Importantly, the combination of GM-CSF with 4-IPP, or with CD74/CXCR7 inhibitors, further enhanced M1-gene expression compared with GM-CSF alone (Figure 5B).

#### Therapeutic evaluation of MØ reprogramming in a MM xenograft model

The above data indicate that MIF is highly detected in the BM microenvironment of MM patient samples (Figure 3), and our in vitro

results established that the most effective treatment of reprogramming M2-MØ toward M1-MØ was the GM-CSF+4-IPP combination (Figure 4). Therefore, we evaluated the potential therapeutic application of this MØ reprogramming combination in NCI-H929 and MM.1S xenograft tumor mouse models. Previously, we confirmed that M-MØ and GM-MØ derived from NSG mice behave similarly to human MØ and that M-MØ repolarized with GM-CSF+4-IPP displayed tumor cytotoxic activity in vitro (supplemental Figure 2I-J). For the NCI-H929 xenografts, cells were subcutaneously injected into NSG and SCID mice, and when tumor volumes reached  $\sim 100 \text{ mm}^3$ , mice were treated with GM-CSF+4-IPP, 4-IPP alone, or vehicle. Significant reductions in NCI-H929 tumor volumes were observed in both murine models treated with GM-CSF+4-IPP, as compared with control mice or to 4-IPP alone (Figure 6A). This effect was not due to MM toxicity, because our in vitro experiments demonstrated that 4-IPP was not toxic for MM cells (supplemental Figure 2K). To assess the specific contribution of MØ in the reduction of MM tumor sizes in mice treated with GM-CSF+4-IPP, we used clodronate-containing liposomes (clo-liposomes) to deplete MØ before the treatment. Subcutaneous NCI-H929 tumors did not develop if clo-liposomes were administered at the time of tumor injection (day 0, data not shown). Therefore, tumors were allowed to develop, and mice were injected intravenously with clo-liposomes when tumors reached  $100 \text{ mm}^3$ . In a preliminary experiment, we observed a significant reduction in TAM 48 hours after clo-liposome administration (data not shown); therefore, GM-CSF+4-IPP treatment was initiated at that time after clo-liposome infusion. Mice treated with GM-CSF+4-IPP developed smaller tumors and survived longer, compared with mice treated with clo-liposomes plus GM-CSF+4-IPP (Figure 6B), suggesting that the presence of MØ during GM-CSF+4-IPP treatment is required for the therapeutic benefit against myeloma.

To further characterize the in vivo reprogramming ability of GM-CSF+4-IPP treatment on SCID murine TAM, tumor-associated myeloid cells were isolated with CD11b magnetic beads from NCI-H929 tumors to quantify the relative expression of a panel of M1 and M2 mouse MØ genes.<sup>46</sup> These analyses revealed a general reduction of M2 markers on treated mice, which was statistically significant for *Cd206*, *Slpr1*, *Stab1*, and *Ctla2b* and was associated with a reciprocal increase in M1 markers, including *Inhba* and *Ccr2*, compared with tumor-bearing control mice (Figure 6C).

For the MM.1S xenograft model, we injected MM.1S-GFP<sup>+</sup> cells intravenously into NSG mice, and after 10 days, animals were treated every 2 days with GM-CSF+4-IPP or vehicle. Upon 2 weeks of treatment, MM.1S infiltration in the BM was quantified by flow cytometry and by messenger RNA expression of human *GAPDH*. The data revealed a significant reduction in MM.1S BM infiltration in GM-CSF+4-IPP-treated mice (Figure 6D-E), which was linked to a decrease in the expression of M2 markers and to an increase in M1 markers, as compared with vehicle (Figure 6F). These data indicate that GM-CSF+4-IPP treatment reprograms gene expression of TAM in vivo and generates a population of MØ with antitumoral properties.

**Figure 6 (continued)** n = 6-10 per group; right, n = 8). (B) NSG mice displaying  $100\text{-mm}^3$  subcutaneous NCI-H929 tumors were injected IV with clodronate, and 2 days later, mice were treated with GM-CSF+4-IPP every 2 days. Tumor growth was measured daily. Data show tumor-volume average of 5 mice per group  $\pm$  SEM. (C) M1 and M2 polarization murine marker expression in CD11b<sup>+</sup> cells isolated from tumors grown in SCID mice, as determined by qRT-PCR (n = 10). Relative expression (log scale) indicates the expression of each marker after GM-CSF+4-IPP treatment relative to its expression in the absence of treatment. (D-E) MM.1S-GFP cells were IV injected into NSG mice, and 10 days later, mice were treated with GM-CSF/4-IPP or with vehicle. Mice were sacrificed after 2 weeks of treatment, and BM cells were analyzed by flow cytometry for human HLA-1 and green fluorescent protein (GFP) expression. Representative dot-plots panels showing HLA-1<sup>+</sup>/GFP<sup>+</sup> percentages (left) and quantification of BM infiltration (right) are displayed. (F) qRT-PCR analyses of human *GAPDH* expression of BM samples from vehicle- or GM-CSF/4-IPP-treated mice. Data show the mean  $\pm$  SEM of 14 mice. (F) M1 and M2 polarization murine marker expression in the BM from NSG mice infiltrated with MM.1S-GFP cells, shown as in (C). mRNA, messenger RNA. \**P* < .05; \*\**P* < .01; \*\*\**P* < .001.

## Discussion

MM remains an incurable malignancy mainly due to minimal residual disease, which is commonly supported by the BM microenvironment, leading to drug resistance and disease relapse.<sup>47</sup> Therefore, new therapeutic strategies that target the supportive microenvironment are urgently needed to boost the efficacy of tumor-directed therapies. TAM represent an abundant component of BM microenvironment that contribute to MM cell resistance to conventional chemotherapy.<sup>4,48</sup> However, the inherent tumoricidal potential of these MØ has not been explored. In the current study, we evaluated for the first time the therapeutic value of reprogramming MØ in MM. We found that MIF is highly expressed in the BM microenvironment and plays an autocrine role in M2-MØ polarization through CD74 and CXCR7. Using a combined treatment to reprogram MM TAM with the pro-M1 cytokine GM-CSF plus blocking the pro-M2 cytokine MIF with 4-IPP, we induced upregulation of M1 markers and the reciprocal downregulation of M2 markers, both in vitro and in vivo. This combined treatment induced MØ-dependent tumor reduction in MM xenograft models, thus identifying MM-MØ as promising therapeutic targets. Furthermore, our data establish the translational potential of combining treatments that promote M1 while simultaneously blocking M2 signaling to re-educate TAM.

We previously described M1 and M2 polarization markers for phenotyping tissue MØ by multicolor confocal microscopy in several human pathologies.<sup>38</sup> Our quantitative image analyses at the single-cell level revealed that TAM from active MM patients have a predominant M2-like phenotype. During tumor evolution, a diverse spectrum of MØ populations develop within the tumor compartment.<sup>49</sup> At early patient diagnosis, MM monocytes/macrophages display a proinflammatory transcriptional profile in the MM microenvironment that leads to transcription of inflammatory cytokines.<sup>6,50</sup> Interestingly, a shift toward M2 polarization occurs upon tumor progression in MM animal models,<sup>50</sup> which is consistent with our results. Indeed, it was recently reported that the levels of soluble CD163 and CD206 (M2-MØ markers) present in serum are independent markers of overall survival in MM patients.<sup>51,52</sup> In addition, we explored other factors reported to control TAM alternative activation, such as MIF, which was selected because it is highly expressed by primary malignant plasma cells.<sup>22,53</sup> Accordingly, we found abundant MIF in the MM BM microenvironment, along with high expression of the MIF receptor CD74 in MM TAM in patient samples. MIF was originally identified as a pro-inflammatory stimulus mainly produced by MØ, which are able to secrete large amounts of this cytokine in response to various stimuli.<sup>54</sup> Nevertheless, MIF is a pleiotropic cytokine with complex context-dependent signaling that leads to inhibition of antitumor reactivity in vivo.<sup>55</sup> Furthermore, MIF controls mature B-cell proliferation and survival, and the humanized anti-CD74 monoclonal Ab milatuzumab is being clinically evaluated for treatment of MM.<sup>56</sup> Thus, blocking MIF or its receptors may target both MM cells and MØ in the BM microenvironment. The dual targeting of MM cells and the BM microenvironment is accomplished by novel therapies, such as bortezomib, thalidomide, and lenalidomide, that have significantly improved patient survival.<sup>57</sup>

As stated above, our goal was to reprogram the M2-like MØ present in the MM microenvironment to become antitumoral M1-like MØ. To this end, we first analyzed the tumoricidal or supportive effects of diverse MØ polarization states toward MM cell lines. Interestingly, M1-like GM-MØ promoted both apoptotic and necrotic forms of programmed cell death to MM cells and limited the growth of MM xenografts in vivo. On the other hand, M-MØ protected MM cells from

bortezomib-induced death in vitro and promoted tumor growth in vivo. Moreover, our previous results showed that M-MØ exhibit a gene profile similar to ex vivo-isolated TAMs from several tumor types,<sup>58</sup> therefore supporting the use of M-MØ as an in vitro TAM model to explore reprogramming protocols.

Reprogramming M-MØ with the pro-M1 cytokine GM-CSF induced low tumoricidal ability compared with GM-MØ programmed from monocytes, indicating that M-MØ are not as plastic as monocyte precursors. To reinforce MØ reprogramming, it is important to block autocrine/paracrine M2 signals, such as M-CSF or MIF, which are abundant in tumor microenvironments and might reverse the reprogrammed “therapeutic” M1-MØ.<sup>19</sup> Inhibition of M-CSF signaling was one of the first TAM targeting strategies, which diminished M2-like MØ programming in glioma.<sup>59</sup> However, blocking M-CSF signaling in combination with GM-CSF to reprogram MØ reduced *INHBA* expression, which encodes Activin A that is a key factor driving GM-CSF-dependent M1 polarization.<sup>33</sup> Interestingly, blocking MIF in combination with GM-CSF showed great induction of *INHBA* expression. MIF has been recently recognized as a pro-M2 tumor-derived factor, whose disruption improved survival in chronic lymphocytic leukemia and melanoma mouse models.<sup>22,27</sup> Our current results extend the role of MIF in M2 polarization from rodent to human MØ and identify CD74 and CXCR7 as the main receptors for MIF involved in a pro-M2-MØ positive feedback mechanism.

Because single pro-M1-MØ or anti-M2-MØ agents had a partial effect in MØ reprogramming, we reasoned that the combination of both treatments may have a synergistic effect. Indeed, treatment with GM-CSF and the MIF-inhibitor 4-IPP showed the best cooperative M1 to M2 shift at gene, protein, and functional levels. Importantly, we demonstrated therapeutic benefit of this novel combination in mouse models of MM that were dependent on MØ. Furthermore, TAM isolated from treated mice displayed enhanced M1 and diminished M2 gene expression. Altogether, our results indicate that MØ-reprogramming strategies may provide significant clinical benefit for MM patients.

## Acknowledgments

The authors gratefully acknowledge Julia Villarejo for technical help. They also thank Mark Penfold from Chemocentryx for providing the high-affinity CXCR7 ligand, CCX733.

This work was supported by the following grants: grant P2010/BMD-2314 from the Comunidad de Madrid (P.S.-M., A.G.-P., J.T., and A.H.); PI13/01454 from Instituto de Salud Carlos III/FEDER (P.S.-M.); RIER RD12/0009 (P.S.-M.), SAF2014-53059-R (J.T.), SAF2012-31613 (A.G.-P.), RD12/0036/0061 (J.T., A.G.-P., and J.M.-L.). The Centro Nacional de Investigaciones Cardiovasculares is supported by the Spanish Ministry of Economy and Competitiveness and the Pro-Centro Nacional de Investigaciones Cardiovasculares Foundation.

## Authorship

Contribution: A.G.-G. designed and performed research, analyzed data, and wrote the manuscript; M.M.-M., R.S., M.R., L.S.-M., and N.A.-S. designed and/or performed research; J.M.-L., A.V., and A.L.C. contributed with vital reagents and materials; J.T., A.G.-P., and A.H. analyzed data and wrote the manuscript; P.S.-M. conceived the study,

designed research, analyzed data, and wrote the manuscript. All the authors approved the final version of the manuscript.

Conflict-of-interest disclosure: The authors declare no competing financial interests.

Correspondence: Paloma Sánchez-Mateos, Instituto de Investigación Sanitaria Gregorio Marañón, Section of Immuno-oncology, Dr Esquerdo 46, 28007 Madrid, Spain; e-mail: paloma.sanchezmateos@salud.madrid.org.

## References

- Raab MS, Podar K, Breitkreutz I, Richardson PG, Anderson KC. Multiple myeloma. *Lancet*. 2009;374(9686):324-339.
- Asimakopoulos F, Kim J, Denu RA, et al. Macrophages in multiple myeloma: emerging concepts and therapeutic implications. *Leuk Lymphoma*. 2013;54(10):2112-2121.
- Kawano Y, Moschetta M, Manier S, et al. Targeting the bone marrow microenvironment in multiple myeloma. *Immunol Rev*. 2015;263(1):160-172.
- Zheng Y, Cai Z, Wang S, et al. Macrophages are an abundant component of myeloma microenvironment and protect myeloma cells from chemotherapy drug-induced apoptosis. *Blood*. 2009;114(17):3625-3628.
- Görgün GT, Whitehill G, Anderson JL, et al. Tumor-promoting immune-suppressive myeloid-derived suppressor cells in the multiple myeloma microenvironment in humans. *Blood*. 2013;121(15):2975-2987.
- Kim J, Denu RA, Dollar BA, et al. Macrophages and mesenchymal stromal cells support survival and proliferation of multiple myeloma cells. *Br J Haematol*. 2012;158(3):336-346.
- Chen H, Campbell RA, Chang Y, et al. Pleiotrophin produced by multiple myeloma induces transdifferentiation of monocytes into vascular endothelial cells: a novel mechanism of tumor-induced vasculogenesis. *Blood*. 2009;113(9):1992-2002.
- Scavelli C, Nico B, Cirulli T, et al. Vasculogenic mimicry by bone marrow macrophages in patients with multiple myeloma. *Oncogene*. 2008;27(5):663-674.
- Suyani E, Sucak GT, Akyürek N, et al. Tumor-associated macrophages as a prognostic parameter in multiple myeloma. *Ann Hematol*. 2013;92(5):669-677.
- Panchabhai S, Kelemen K, Ahmann G, et al. Tumor-associated macrophages and extracellular matrix metalloproteinase inducer in prognosis of multiple myeloma. *Leukemia*. 2016;30(4):951-954.
- Kim D, Wang J, Willingham SB, Martin R, Wernig G, Weissman IL. Anti-CD47 antibodies promote phagocytosis and inhibit the growth of human myeloma cells. *Leukemia*. 2012;26(12):2538-2545.
- Haabeth OA, Tveita AA, Fauskanger M, et al. How do CD4(+) T cells detect and eliminate tumor cells that either lack or express MHC class II molecules? *Front Immunol*. 2014;5:174.
- Jensen JL, Rakhmievich A, Heninger E, et al. Tumorcidal effects of macrophage-activating immunotherapy in a murine model of relapsed/refractory multiple myeloma. *Cancer Immunol Res*. 2015;3(8):881-890.
- Sica A, Mantovani A. Macrophage plasticity and polarization: in vivo veritas. *J Clin Invest*. 2012;122(3):787-795.
- Martinez FO, Gordon S. The M1 and M2 paradigm of macrophage activation: time for reassessment. *F1000Prime Rep*. 2014;6:13.
- Jaiswal S, Chao MP, Majeti R, Weissman IL. Macrophages as mediators of tumor immunosurveillance. *Trends Immunol*. 2010;31(6):212-219.
- Feng M, Chen JY, Weissman-Tsukamoto R, et al. Macrophages eat cancer cells using their own calreticulin as a guide: roles of TLR and Btk. *Proc Natl Acad Sci USA*. 2015;112(7):2145-2150.
- Biswas SK, Mantovani A. Macrophage plasticity and interaction with lymphocyte subsets: cancer as a paradigm. *Nat Immunol*. 2010;11(10):889-896.
- Noy R, Pollard JW. Tumor-associated macrophages: from mechanisms to therapy [published correction appears in *Immunity*. 2014;41(5):866]. *Immunity*. 2014;41(1):49-61.
- Ries CH, Cannarile MA, Hoves S, et al. Targeting tumor-associated macrophages with anti-CSF-1R antibody reveals a strategy for cancer therapy. *Cancer Cell*. 2014;25(6):846-859.
- Bronte V, Murray PJ. Understanding local macrophage phenotypes in disease: modulating macrophage function to treat cancer. *Nat Med*. 2015;21(2):117-119.
- Yaddanapudi K, Putty K, Rendon BE, et al. Control of tumor-associated macrophage alternative activation by macrophage migration inhibitory factor. *J Immunol*. 2013;190(6):2984-2993.
- Simpson KD, Templeton DJ, Cross JV. Macrophage migration inhibitory factor promotes tumor growth and metastasis by inducing myeloid-derived suppressor cells in the tumor microenvironment. *J Immunol*. 2012;189(12):5533-5540.
- Hume DA, MacDonald KP. Therapeutic applications of macrophage colony-stimulating factor-1 (CSF-1) and antagonists of CSF-1 receptor (CSF-1R) signaling. *Blood*. 2012;119(6):1810-1820.
- Legendre H, Decaestecker C, Nagy N, et al. Prognostic values of galectin-3 and the macrophage migration inhibitory factor (MIF) in human colorectal cancers. *Mod Pathol*. 2003;16(5):491-504.
- Schulz R, Marchenko ND, Holembowski L, et al. Inhibiting the HSP90 chaperone destabilizes macrophage migration inhibitory factor and thereby inhibits breast tumor progression [published correction appears in *J Exp Med*. 2012;209(3):640]. *J Exp Med*. 2012;209(2):275-289.
- Reinart N, Nguyen PH, Boucas J, et al. Delayed development of chronic lymphocytic leukemia in the absence of macrophage migration inhibitory factor. *Blood*. 2013;121(5):812-821.
- Samaniego R, Palacios BS, Domínguez-Soto A, et al. Macrophage uptake and accumulation of folates are polarization-dependent in vitro and in vivo and are regulated by activin A. *J Leukoc Biol*. 2014;95(5):797-808.
- Buechler C, Ritter M, Orsó E, Langmann T, Klucken J, Schmitz G. Regulation of scavenger receptor CD163 expression in human monocytes and macrophages by pro- and antiinflammatory stimuli. *J Leukoc Biol*. 2000;67(1):97-103.
- Puig-Kröger A, Sierra-Filardi E, Domínguez-Soto A, et al. Folate receptor beta is expressed by tumor-associated macrophages and constitutes a marker for M2 anti-inflammatory/regulatory macrophages. *Cancer Res*. 2009;69(24):9395-9403.
- Estecha A, Aguilera-Montilla N, Sánchez-Mateos P, Puig-Kröger A. RUNX3 regulates intercellular adhesion molecule 3 (ICAM-3) expression during macrophage differentiation and monocyte extravasation. *PLoS One*. 2012;7(3):e33313.
- Escribese MM, Sierra-Filardi E, Nieto C, et al. The prolyl hydroxylase PHD3 identifies proinflammatory macrophages and its expression is regulated by activin A. *J Immunol*. 2012;189(4):1946-1954.
- Sierra-Filardi E, Puig-Kröger A, Blanco FJ, et al. Activin A skews macrophage polarization by promoting a proinflammatory phenotype and inhibiting the acquisition of anti-inflammatory macrophage markers. *Blood*. 2011;117(19):5092-5101.
- Urban JL, Shepard HM, Rothstein JL, Sugarman BJ, Schreiber H. Tumor necrosis factor: a potent effector molecule for tumor cell killing by activated macrophages. *Proc Natl Acad Sci USA*. 1986;83(14):5233-5237.
- Tugues S, Burkhard SH, Ohs I, et al. New insights into IL-12-mediated tumor suppression. *Cell Death Differ*. 2015;22(2):237-246.
- Lee C, Oh JI, Park J, et al. TNF alpha mediated IL-6 secretion is regulated by JAK/STAT pathway but not by MEK phosphorylation and AKT phosphorylation in U266 multiple myeloma cells. *Biomed Res Int*. 2013;2013:580135.
- Takaku T, Malide D, Chen J, Calado RT, Kajigaya S, Young NS. Hematopoiesis in 3 dimensions: human and murine bone marrow architecture visualized by confocal microscopy. *Blood*. 2010;116(15):e41-e55.
- González-Domínguez É, Samaniego R, Flores-Sevilla JL, et al. CD163L1 and CLEC5A discriminate subsets of human resident and inflammatory macrophages in vivo. *J Leukoc Biol*. 2015;98(4):453-466.
- Leng L, Metz CN, Fang Y, et al. MIF signal transduction initiated by binding to CD74. *J Exp Med*. 2003;197(11):1467-1476.
- Conway JG, McDonald B, Parham J, et al. Inhibition of colony-stimulating-factor-1 signaling in vivo with the orally bioavailable cFMS kinase inhibitor GW2580. *Proc Natl Acad Sci USA*. 2005;102(44):16078-16083.
- Winner M, Meier J, Zierow S, et al. A novel, macrophage migration inhibitory factor suicide substrate inhibits motility and growth of lung cancer cells. *Cancer Res*. 2008;68(18):7253-7257.
- Bai F, Asojo OA, Cirillo P, et al. A novel allosteric inhibitor of macrophage migration inhibitory factor (MIF). *J Biol Chem*. 2012;287(36):30653-30663.
- Kelly B, O'Neill LA. Metabolic reprogramming in macrophages and dendritic cells in innate immunity. *Cell Res*. 2015;25(7):771-784.
- Sag D, Carling D, Stout RD, Suttles J. Adenosine 5'-monophosphate-activated protein kinase promotes macrophage polarization to an anti-inflammatory functional phenotype. *J Immunol*. 2008;181(12):8633-8641.
- Bernhagen J, Krohn R, Lue H, et al. MIF is a noncognate ligand of CXC chemokine receptors in inflammatory and atherogenic cell recruitment. *Nat Med*. 2007;13(5):587-596.
- de las Casas-Engel M, Domínguez-Soto A, Sierra-Filardi E, et al. Serotonin skews human macrophage polarization through HTR2B and HTR7. *J Immunol*. 2013;190(5):2301-2310.
- Bianchi G, Richardson PG, Anderson KC. Promising therapies in multiple myeloma. *Blood*. 2015;126(3):300-310.

48. Zheng Y, Yang J, Qian J, et al. PSGL-1/ selectin and ICAM-1/CD18 interactions are involved in macrophage-induced drug resistance in myeloma. *Leukemia*. 2013;27(3):702-710.
49. Qian BZ, Pollard JW. Macrophage diversity enhances tumor progression and metastasis. *Cell*. 2010;141(1):39-51.
50. Hope C, Ollar SJ, Heninger E, et al. TPL2 kinase regulates the inflammatory milieu of the myeloma niche. *Blood*. 2014;123(21):3305-3315.
51. Andersen MN, Abildgaard N, Maniecki MB, Møller HJ, Andersen NF. Monocyte/macrophage-derived soluble CD163: a novel biomarker in multiple myeloma. *Eur J Haematol*. 2014;93(1):41-47.
52. Andersen MN, Andersen NF, Rødggaard-Hansen S, Hokland M, Abildgaard N, Møller HJ. The novel biomarker of alternative macrophage activation, soluble mannose receptor (sMR/sCD206): Implications in multiple myeloma. *Leuk Res*. 2015;39(9):971-975.
53. Claudio JO, Masih-Khan E, Tang H, et al. A molecular compendium of genes expressed in multiple myeloma. *Blood*. 2002;100(6):2175-2186.
54. Calandra T, Roger T. Macrophage migration inhibitory factor: a regulator of innate immunity. *Nat Rev Immunol*. 2003;3(10):791-800.
55. Zhou Q, Yan X, Gershan J, Orentas RJ, Johnson BD. Expression of macrophage migration inhibitory factor by neuroblastoma leads to the inhibition of antitumor T cell reactivity in vivo. *J Immunol*. 2008;181(3):1877-1886.
56. Starlets D, Gore Y, Binsky I, et al. Cell-surface CD74 initiates a signaling cascade leading to cell proliferation and survival. *Blood*. 2006;107(12):4807-4816.
57. Kumar SK, Rajkumar SV, Dispenzieri A, et al. Improved survival in multiple myeloma and the impact of novel therapies. *Blood*. 2008;111(5):2516-2520.
58. Soler Palacios B, Estrada-Capetillo L, Izquierdo E, et al. Macrophages from the synovium of active rheumatoid arthritis exhibit an activin A-dependent pro-inflammatory profile. *J Pathol*. 2015;235(3):515-526.
59. Pyonteck SM, Akkari L, Schuhmacher AJ, et al. CSF-1R inhibition alters macrophage polarization and blocks glioma progression. *Nat Med*. 2013;19(10):1264-1272.